On the formation of highly oxidized pollutants by autoxidation of terpenes under low temperature combustion conditions: the case of limonene and α-pinene.

Roland Benoit[1], Nesrine Belhadj[1,2], Zahraa Dbouk[1,2], Maxence Lailliau[1,2], and Philippe Dagaut[1]

[1]CNRS-INSIS, ICARE, Orléans, France, roland.benoit@cnrs-orleans.fr, nesrine.belhadj@cnrs-orleans.fr, zahraa.dbouk@cnrs-orleans.fr, maxence.lailliau@cnrs-orleans.fr, dagaut@cnrs-orleans.fr
[2]Université d'Orléans, Orléans, France

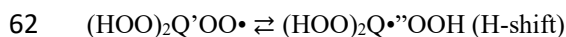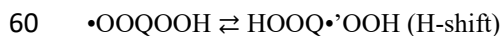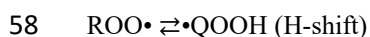**Correspondance**: Roland Benoit (roland.benoit@cnrs-orleans.fr)

Abstract.

The oxidation of monoterpenes under atmospheric conditions has been the subject of numerous studies. They were motivated by the formation of oxidized organic molecules (OOM) which, due to their low vapor pressure, contribute to the formation of secondary organic aerosols (SOA). Among the different reaction mechanisms proposed for the formation of these oxidized chemical compounds, it appears that the autoxidation mechanism, involving successive events of O_2 addition and H-migration, common to both low-temperature combustion and atmospheric conditions, is leading to the formation of highly oxidized products (HOPs). However, cool flame oxidation (~500-800 K) of terpenes has not received much attention even if it can contribute to atmospheric pollution through biomass burning and wildfires. Under such conditions, terpenes can be oxidized via autoxidation. In the present work, we performed oxidation experiments with limonene-oxygen-nitrogen and α-pinene-oxygen-nitrogen mixtures in a jet-stirred reactor (JSR) at 590 K, a residence time of 2 s, and atmospheric pressure. Oxidation products were analyzed by liquid chromatography, flow injection, and soft ionization-high resolution mass spectrometry. H/D exchange and 2,4-dinitrophenyl hydrazine derivatization were used to assess the presence of OOH and C=O groups in oxidation products, respectively. We probed the effects of the type of ionization used in mass spectrometry analyses on the detection of oxidation products. Heated electrospray ionization (HESI) and atmospheric pressure chemical ionization (APCI), in positive and negative modes were used. We built an experimental database consisting of literature data for atmospheric oxidation and presently obtained combustion data for the oxidation of the two selected terpenes. This work showed a surprisingly similar set of oxidation products chemical formulas, including oligomers, formed under the two rather different conditions, i.e., cool flame and simulated atmospheric oxidation. Data analysis (in HESI mode) indicated that a subset of chemical formulas is common to all experiments, independently of experimental conditions. Finally, this study indicates that more than 45% of the detected chemical formulas in this full dataset can be ascribed to an autoxidation reaction.

33 **1 Introduction**

34 Terpenes are emitted into the troposphere by vegetation (Seinfeld and Pandis, 2006). They can be used as drop in fuels

35 (Harvey et al., 2010;Mewalal et al., 2017;Harvey et al., 2015) which could increase emissions via fuel evaporation

36 and unburnt fuel release. Biomass burning and wildfires can also release terpenes and their products of oxidation into

37 the troposphere (Gilman et al., 2015;Hatch et al., 2019;Schneider et al., 2022). Wildfires temperature ranges from 573

38 to 1373 K (Wotton et al., 2012), which covers both the cool flame (~500-800 K) and intermediate to high temperature

39 combustion regimes. Products of biomass burning have been characterized earlier (Smith et al., 2009). Using van

40 Krevelen diagrams, the authors reported H/C versus O/C in the ranges 0.5 to 3 and 0 to 1, respectively. Whereas a

41 large fraction of these products can derive from cellulose, hemicellulose, and lignin oxidation, their formation via

42 terpenes oxidation cannot be ruled out. In a more recent study (Gilman et al., 2015), it was reported that biomass

43 burning emissions were dominated by oxidized organic compounds (57 to 68% of total mass emissions). Wildfires

44 are getting more and more frequent and their intensity increases(Burke et al., 2021). In large wildfires, there are many

45 updrafts which can transport a variety of materials ranging from gases to particulates, and even bacteria (Kobziar et

46 al., 2018). Furthermore, it was recently demonstrated that recent wildfires in Australia produced smoke which could

47 reach an altitude of 35 km (Khaykin et al., 2020). Such events could contribute to ozone destruction (Bernath et al.,

48 2022) but also to tropospheric pollution. But, field measurements are not appropriate for comparison with the present

49 data because a strict distinction on the origins of the chemical compounds observed cannot be assessed. For example,

50 literature works and reviews (Hu et al., 2018;Popovicheva et al., 2019;Prichard et al., 2020) present field measurements

51 from smoldering fires which were not detailed enough to be used here.

52 Cool flame oxidation is dominated by autoxidation (Bailey and Norrish, 1952;Benson, 1981;Cox and Cole,

53 1985;Korcek et al., 1972) which involves peroxy radicals (ROO$^\bullet$). Autoxidation is based on an H-shift and oxygen

54 addition which starts with the initial production of ROO$^\bullet$ radicals. This mechanism can repeat itself several times and

55 lead to recurrent oxygen additions to form highly oxidized products (Wang et al., 2017;Wang et al., 2018;Belhadj et

56 al., 2020;Belhadj et al., 2021a;Belhadj et al., 2021b):

57 R$\bullet$+ O$_2$ $\rightleftarrows$ ROO$\bullet$ (first O$_2$-addition)

58 ROO$\bullet$ $\rightleftarrows$$\bullet$QOOH (H-shift)

59 $\bullet$QOOH +O$_2$ $\rightleftarrows$ $\bullet$OOQOOH (second O$_2$-addition)

60 $\bullet$OOQOOH $\rightleftarrows$ HOOQ$\bullet$'OOH (H-shift)

61 HOOQ$\bullet$'OOH +O$_2$ $\rightleftarrows$ (HOO)$_2$Q'OO$\bullet$ (third O$_2$-addition)

62 (HOO)$_2$Q'OO$\bullet$ $\rightleftarrows$ (HOO)$_2$Q$\bullet$''OOH (H-shift)

63 (HOO)$_2$Q$\bullet$''OOH +O$_2$ $\rightleftarrows$ (HOO)$_3$Q''OO$\bullet$ (fourth O-addition), etc.

64 There, the formation of highly oxidized products (HOPs) was mainly attributed to autoxidation reactions (Belhadj et

65 al., 2021c;Benoit et al., 2021).

66 In atmospheric chemistry, it is only relatively recently that this pathway has been considered (Vereecken et al.,

67 2007;Crounse et al., 2013;Jokinen et al., 2014a;Ehn et al., 2014;Berndt et al., 2015;Jokinen et al., 2015;Berndt et al.,

68 2016;Iyer et al., 2021). Also, it has been identified that highly oxygenated organic molecules (HOMs), a source of

69 secondary organic aerosols (SOA), can result from autoxidation processes (Ehn et al., 2014;Wang et al., 2021;Tomaz

70 et al., 2021;Bianchi et al., 2019). Modeling studies complemented by laboratory experiments showed that autoxidation

71 mechanisms proceed simultaneously on different ROO$^{\bullet}$ radicals leading to the production of a wide range of oxidized
72 compounds in a few hundredths of a second (Jokinen et al., 2014a;Berndt et al., 2016;Bianchi et al., 2019;Iyer et al.,
73 2021). Recent works have shown that, under certain atmospheric conditions, this autoxidation mechanism could be
74 competitive with other reaction pathways involving ROO$^{\bullet}$ radicals (Bianchi et al., 2019), e.g., the carbonyl channel
75 (ROO$^{\bullet} \to$ R$_{-H}$O + OH), the hydroperoxide channel (ROO$^{\bullet}$ + HOO$^{\bullet} \to$ ROOH + O$_2$ and RO$^{\bullet}$ + $^{\bullet}$OH + O$_2$),
76 disproportionation reactions (ROO$^{\bullet}$ + R'OO$^{\bullet} \to$ RO$^{\bullet}$ + R'O$^{\bullet}$ + O$_2$ and R$_{-H}$O + R'OH + O$_2$), accretion reactions (ROO$^{\bullet}$
77 + R'OO$^{\bullet} \to$ ROOR' + O$_2$). Similarity, in terms of observed chemical formulas of products from cool flame oxidation
78 of limonene and atmospheric oxidation of limonene, has been reported recently (Benoit et al., 2021). The same year,
79 Wang et al. showed that the oxidation of alkanes follows this autoxidation mechanism under both atmospheric and
80 combustion conditions (Wang et al., 2021). Also, that work confirmed that internal H-shifts in autoxidation can be
81 promoted by the presence of functional groups, as predicted earlier (Otkjær et al., 2018) for ROO$^{\bullet}$ radicals containing
82 OOH, OH, OCH$_3$, CH$_3$, C=O, or C=C groups. Autoxidation will preferentially form chemical functions such as
83 carbonyls, hydroperoxyl, or peroxyl. This large diversity of chemical functions will promote the formation of isomers.
84 Nevertheless, the common point to these chemical compounds is the sequential addition of O$_2$. Therefore, in a database,
85 potential candidate products of autoxidation are easily identified by this sequential addition.

86 To better understand the importance of these reaction pathways, the experimental conditions unique to these two
87 chemistries must be considered. In laboratory studies conducted under simulated atmospheric conditions, oxidation
88 occurs at near-ambient temperatures (250-300 K), at atmospheric pressure, in the presence of ozone and/or $^{\bullet}$OH
89 radicals (Table S1), used to initiate oxidation with low initial terpene concentrations. In combustion, the $^{\bullet}$OH radical,
90 temperature, and pressure are driving autoxidation. In addition to the increase in temperature, the initial concentrations
91 of the reagents are generally higher compared to the atmospheric conditions, in order to initiate the oxidation with O$_2$,
92 which is much slower than that involving ozone or $^{\bullet}$OH. Rising temperature increases isomerization rates and favors
93 autoxidation, at the expense of other possible reactions of ROO$^{\bullet}$ radicals. Indeed, it has been reported earlier that a
94 temperature rise from 250 to 273K does not affect the distribution of HOMs (Quéléver et al., 2019) whereas Tröstl et
95 al. suggested that the distribution of HOMs is affected by temperature, α-pinene or particle concentration (Tröstl et al.,
96 2016). Similarly, the experiments of Huang et al. performed at different temperatures (223 K and 296 K) and precursor
97 concentration (α-pinene 0.714 and 2.2 ppm) suggested that the physicochemical properties, such as the composition
98 of the oligomers (at the nanometer scale), can be affected by a variation of temperature (Huang et al., 2018). The broad
99 range of chemical molecules formed and the impact of the experimental conditions on their character remains a subject
100 for atmospheric chemistry as well as for combustion chemistry studies. Whatever the mechanism of aerosols
101 formation, i.e., oligomerization, functionalization, or accretion, their composition will be linked to that of the initial
102 radical pool (Camredon et al., 2010;Meusinger et al., 2017;Tomaz et al., 2021).

103 In low-temperature combustion, when the temperature is increased, fuel's autoxidation rate goes through a maximum
104 between 500 and 670 K, depending on the nature of the fuel (Belhadj et al., 2020;Belhadj et al., 2021c). In low-
105 temperature combustion chemistry as in atmospheric chemistry, the oxidation of a chemical compound leads to the
106 formation of several thousands of chemical products which result from successive additions of oxygen, isomerization,
107 accretion, fragmentation, and oligomerization (Benoit et al., 2021;Belhadj et al., 2021b). The exhaustive analysis of
108 chemical species remains, under the current instrumental limitations, impossible. Indeed, this would consist in
109 analyzing several thousands of molecules using separative techniques such as ultra-high-pressure liquid
110 chromatography (UHPLC) or ion mobility spectrometry (IMS) (Krechmer et al., 2016;Kristensen et al., 2016).

111 Nevertheless, it is possible to classify these molecular species, considering only $C_xH_yO_z$ compounds, according to

112 criteria accessible via graphic tools representation such as van Krevelen diagrams, double bond equivalent number

113 (DBE), and average carbon oxidation state (OSc) versus the number of carbon atoms (Kourtchev et al., 2015;Nozière

114 et al., 2015). Such postprocessing of large datasets has the advantage of immediately highlighting classes of

115 compounds or physicochemical properties such as the condensation of molecules (vapor pressure), the large variety

116 of oxidized products ($C_xH_yO_{1 \text{ to } 15}$ in the present experiments) and the formation of oligomers (Kroll et al., 2011;Xie et

117 al., 2020).

118 In addition to the recent studies focusing on the first steps of autoxidation, a more global approach, based on the

119 comparison of possible chemical transformations related to autoxidation in low temperature combustion and

120 atmospheric chemistry, is needed for evaluating the importance of autoxidation under tropospheric and low-

121 temperature combustion conditions. In order to study the effects of experimental conditions on the diversity of

122 chemical molecules formed by autoxidation, we have selected α-pinene and limonene, two isomeric terpenes among

123 the most abundant in the troposphere (Zhang et al., 2018). Limonene has a single ring structure and two double bonds,

124 one of which is exocyclic. α-Pinene has a bicyclic structure and a single endo-cyclic double bond. These two isomers

125 with their distinctive physicochemical characters are good candidates for studying autoxidation versus initial chemical

126 structure and temperature. For α-pinene, in addition to the reactivity of its endo-cyclic double bond, products of ring

127 opening of the cyclobutyl group have been detected (Kurtén et al., 2015;Iyer et al., 2021), which could explain the

128 diversity of observed oxidation products. This large pool of oxidation products is increased in the case of limonene by

129 the presence of two double bonds (Hammes et al., 2019;Jokinen et al., 2015).

130 The present work extends that concerning the oxidation of limonene alone (Benoit et al., 2021). Compared to previous

131 works, we have added the study of α-pinene oxidation to that of limonene and investigated the impact of ionization

132 modes on the number of molecules detected and their chemical nature (unsaturation, oxidation rate). The size of the

133 experimental and bibliographic databases has been increased by more than 50%, in particular by adding data specific

134 to autoxidation (Krechmer et al., 2016;Tomaz et al., 2021) and references on α-pinene (Tab. 2)). Here, we oxidized

135 α-pinene and limonene in a jet-stirred reactor at atmospheric pressure, excess of oxygen, and elevated temperature.

136 We characterized the impact of using different ionization techniques (HESI and APCI) in positive and negative modes

137 on the pool of detected chemical formulas. The particularities of each ionization mode were analyzed to identify the

138 most suitable ionization technique for exploring the formation of autoxidation products under low temperature

139 combustion. H/D exchange and 2,4-dinitrophenyl hydrazine derivatization were used to assess the presence of

140 hydroperoxy and carbonyl groups, respectively. Chemical formulas detected here and in atmospheric chemistry studies

141 were compiled and tentatively used to evaluate the importance of autoxidation routes under both conditions.

142 **2 Experiments**

143 **2.1 Oxidation experiments**

144 The present experiments were carried out in a fused silica jet-stirred reactor (JSR) setup presented earlier (Dagaut et

145 al., 1986;Dagaut et al., 1988) and used in previous studies (Dagaut et al., 1987;Benoit et al., 2021;Belhadj et al.,

146 2021c). We studied separately the oxidation of the two isomers, α-pinene and limonene. As in earlier works (Benoit

147 et al., 2021;Belhadj et al., 2021c), α-pinene (+), 98% pure from Sigma Aldrich and limonene (R)-(+), >97% pure from

148 Sigma Aldrich, were pumped by an HPLC pump (Shimadzu LC10 AD VP) with an online degasser (Shimadzu DGU-

149 20 A3) and sent to a vaporizer assembly where it was diluted by a nitrogen flow. Each terpene isomer and oxygen,

150 both diluted by N_2, were sent separately to a 42 mL JSR to avoid oxidation before reaching 4 injectors (nozzles of 1

151 mm I.D.) providing stirring. The flow rates of nitrogen and oxygen were controlled by mass flow meters. Good thermal

152 homogeneity along the vertical axis of the JSR was recorded (gradients of < 1 K/cm) by thermocouple measurements

153 (0.1 mm Pt-Pt/Rh-10% wires located inside a thin-wall silica tube). In order to observe the oxidation of these isomers,

154 which are not prone to strong self-ignition, the oxidation of 1% of these chemical compounds ($C_{10}H_{16}$) under fuel-lean

155 conditions (equivalence ratio 0.25, 56% O_2, 43% N_2), was carried out at 590 K, atmospheric pressure, and a residence

156 time of 2 s. Under these conditions, the oxidation of the two isomers is initiated by slow H-atom abstraction by

157 molecular oxygen ($RH + O_2 \rightarrow R^\bullet + HO_2^\bullet$). The fuel radicals $R^\bullet$ react rapidly with O_2 to form peroxy radicals which

158 undergo further oxidation, characteristic of autoxidation. Nevertheless, this autoxidation mechanism, although

159 predominant, is not exclusive and other oxidation mechanisms are possible (Belhadj et al., 2021b). In this case, there

160 may be a random overlap of chemical formulas. The autoxidation criteria (two chemical formulas separated by two

161 oxygen atoms) allows to limit or avoid these overlaps.

2.2 Chemical analyses

163 A 2 mm I.D. probe was used to collect samples. To measure low-temperature oxidation products ranging from early

164 oxidation steps to highly oxidized products, the samples were bubbled into cooled acetonitrile (UHPLC grade ≥99.9,

165 T= 0°C, 250 mL) for 90 min. The resulting solution was stored in a freezer at -15°C. The stability of the products was

166 verified. No detectable changes in the mass spectra were observed after more than one month which is consistent with

167 previous findings (Belhadj et al., 2021c).

168 Analyses of samples collected in acetonitrile (ACN) were carried out via direct infusion (rate: 3μL/min and recorded

169 for 1 min for data averaging) in the ionization chamber of a high-resolution mass spectrometer (Thermo Scientific

170 Orbitrap® Q-Exactive, mass resolution 140,000 and mass accuracy <0.5 ppm RMS). UHPLC conditions were: a

171 Vanquish UHPLC Thermo Fisher Scientific with a C18 column (Phenomenex Luna, 1.6 μm, 110 Å, 100x2.1 mm).

172 The column temperature was maintained at 40°C. 3μml of sample were eluted by a mobile phase containing water-

173 ACN mix (pure water, ACN HPLC grade) at a flow rate of 250 μL/min (gradient: 5% to 20% ACN -3 min, 20% to

174 65% ACN - 22 min, 65% to 75% ACN – 4 min, 75% to 90% ACN - 4 min, for a total of 33 min).

175 Both heated electrospray ionization (HESI) and atmospheric chemical ionization (APCI) were used in positive and

176 negative modes for the ionization of products. HESI settings were: spray voltage 3.8 kV, vaporizer temperature of

177 150°C, capillary temperature 200°C, sheath gas flow of 8 arbitrary units (a.u.), auxiliary gas flow of 1 a.u., sweep gas

178 flow of 0 a.u.. In APCI, settings were: corona discharge current of 3μA, spray voltage 3.8 kV, vaporizer temperature

179 of 150°C, capillary temperature of 200°C, sheath gas flow of 8 a.u., auxiliary gas flow of 1 a.u., sweep gas flow of 0

180 a.u.. In order to avoid transmission and detection effects of ions depending on their mass inside the C-Trap (Hecht et

181 al., 2019), acquisitions with three mass ranges were performed (m/z 50-750; m/z 150-750; m/z 300-750). The upper

182 limit of m/z 750 was chosen because of the absence of a signal beyond this value. It was shown that no significant

183 oxidation occurred in the HESI and APCI ion sources by injecting a limonene-ACN mixture (Fig. S1). The

184 optimization of the Orbitrap ionization parameters in HESI and APCI did not show any clustering phenomenon for

185 these two monoterpene isomers. The parameters evaluated were: injection source - capillary distance, vaporization

and capillary temperatures, applied difference of potential, injected volume, flow rate of nitrogen in the ionization source. Positive and negative HESI mass calibrations were performed using Pierce^{TM} calibration mixtures (Thermo Scientific). Chemical compounds with relative intensity less than 1 ppm to the highest MS signal in the mass spectrum were not considered. Nevertheless, it should be considered that some of the molecules presented in this study could result from our experimental conditions (continuous flow reactor, reagent concentration, temperature, reaction time) and to some extent from our acquisition conditions, different from those in the previous studies (Deng et al., 2021;Quéléver et al., 2019;Meusinger et al., 2017;Krechmer et al., 2016;Tomaz et al., 2021;Fang et al., 2017;Witkowski and Gierczak, 2017;Jokinen et al., 2015;Nørgaard et al., 2013;Bateman et al., 2009;Walser et al., 2008;Warscheid and Hoffmann, 2001;Hammes et al., 2019;Kundu et al., 2012). Operating with a continuous flow reactor at elevated temperature and high initial concentration of reagents allows the formation of combustion-relevant products, which does not exclude their possible formation under atmospheric conditions. To assess the formation of products containing OOH and C=O groups, as in previous works (Belhadj et al., 2021a;Belhadj et al., 2021b), H/D exchange with D_2O and 2,4-dinitrophenyl hydrazine derivation were used, respectively.

3 Data Processing

High resolution mass spectrometry (HR-MS) generates large datasets which are difficult to fully analyze by sequential methods. When the study requires the processing of several thousands of molecules, the use of statistical tools and graphical representation means becomes necessary. In this study, we have chosen to use the van Krevelen diagram (Van Krevelen, 1950) by adding an additional dimension, the double bond equivalent (DBE). The DBE number represents the sum of unsaturation and rings present in a chemical compound (Melendez-Perez et al., 2016). The interest of this type of representation is to be able to identify more easily the clusters (increase of the DBE number at constant O/C and H/C ratios)

$$DBE = 1 + C - H/2$$

This number is independent of the number of O-atoms, but changes with the number of hydrogen atoms. Decimal values of this number, which correspond to an odd number of hydrogen atoms, were not considered in this study. Then, the superpositions of points (and therefore of chemical formulas) in the O/C vs. H/C space are suppressed. The oxidation state of carbon (OSc) provides a measure of the degree of oxidation of chemical compounds (Kroll et al., 2011). This provides a framework for describing the chemistry of organic species. It is defined by the following equation:

$$OSc \approx 2\,O/C - H/C$$

4 Results and discussion

We studied the oxidation of α-pinene and limonene ($C_{10}H_{16}$) at 590 K, under atmospheric pressure, with a residence time of 2 s, and a fuel concentration of 1%. Under these conditions, the formation of peroxides by autoxidation at low temperature should be efficient (Belhadj et al., 2021c), even though the conversion of the fuels remains moderate.

4.1 Characterization of ionization sources

First, we have studied the impact of APCI and HESI sources, in positive and negative modes, on the chemical formulas detected. The HESI and APCI sources in positive and negative mode were used and their operating parameters were varied, i.e., temperature, gas flow and accelerating voltage (see Section 2). For each polarity, only ions composed of carbon, hydrogen (even numbers) and oxygen were considered. Molecular duplicates inherent to mass range overlaps were excluded. By following these rules, we obtained a different number of ions depending on the ionization source and the polarity used. Table 1 shows the number of ions according to the experimental conditions and the discrimination rules.

Table 1. Number of ions detected for each source in positive and negative modes (by protonation or deprotonation, respectively)

Ionization source	α-Pinene		Limonene	
APCI	646 $(R+H)^+$	503 $(R–H)^–$	1321 $(R+H)^+$	1346 $(R–H)^–$
HESI	594 $(R+H)^+$	693 $(R–H)^–$	1017 $(R+H)^+$	1864 $(R–H)^–$

Each combination of ionization sources and polarity generated a set of chemical formulas. To make a meaningful comparison between the positive and negative ions data, the chemical formulas used were the precursors of the ions identified in the mass spectra. These sets have common data, but also specific chemical formulas. For a given ionization source, ~ 50% of the chemical formulas are observed whatever the ionization polarity, i.e., using both polarities one can capture between 30-50% more molecular species (since some of them are ionized under a single mode (+ or –) depending on their chemical structure). Utilizing both ionization polarities is helpful for identifying a larger quantity of species. The HESI source data were compared to the APCI data (Supplement, Tables S1 and S2), showing an increased number (20 to 30%) of chemical formulas detected by HESI. This increase is characterized by a better detection of negatively ionized species and those with a higher DBE. In order to evaluate further the interest for using these ionization sources, we compiled these data in Venn diagrams and proposed a visualization of these sets with a van Krevelen representation; we added the number of DBE in the third dimension (Supplement, Tables S1 and S2).

In positive ionization mode, independently of the ionization source and in addition to the common molecular formulas, we detected products with an O/C ratio < 0.2 whereas in the negative ionization mode, we detected molecular formulas with an O/C ratio > 0.5. In addition to these observations, we noted that HESI is more appropriate for studying products with a large number of unsaturation (DBE > 5), which is probably related to the increase in the number of hydroperoxide and carboxyl groups along with the fact that a heated ionization source favors vaporization of low volatility compounds. Finally, for an optimal detection of the oxidation products, it is necessary to consider the transmission limits of the C-Trap. Here, we could increase by more than 60% the number of molecular formulas detected using several mass ranges for data acquisition (section 2.2). The most appropriate ionization polarity to be used is tied to chemical functions present in products to be detected. We could increase by 30 to 100% the number of chemical formulas detected by using both positive and negative ionization modes. Using HESI is consistent with previous findings indicating ESI is well suited for the ionization of acidic, polar, and heteroatom-containing chemicals (Kekäläinen et al., 2013). To illustrate the present results, HESI (–)-MS spectra are provided in the Supplement (Fig.

254 S2). The list of all chemical formulas found in limonene and α-pinene samples (HESI negative and positive mode) is
255 given in the data-supplement file

256

4.2 Autoxidation products detected in a JSR

258 In order to compare the oxidation of α-pinene and limonene, we compiled the positive and negative ionization data
259 obtained with APCI (Table S1) and HESI (Table S2) ionization sources to obtain a more exhaustive database. For the
260 APCI and HESI sources, we distinguished three datasets, two of which are specific to the oxidation of α-pinene and
261 limonene and one which is common to both isomers. In the following text, "only" will be used to describe the
262 molecules specific to the oxidation of one of the isomeric terpenes. This common dataset represents more than 90%
263 of the chemical formulas identified in the α-pinene oxidation samples detected with APCI or HESI. For limonene, for
264 which the number of identified chemical formulas is larger, regardless of the ionization source, this common data set
265 represents nearly 40% of the chemical formulas detected. In these two cases, the relatively low residence time (2
266 seconds) and the diversity of the chemical formulas obtained suggest that the oxidation of these two terpene isomers
267 leads to ring opening, a phenomenon also observed in atmospheric chemistry (Berndt et al., 2016;Zhao et al., 2018;Iyer
268 et al., 2021). Concerning the molecular formulas of products common to both isomers, Figure 1 shows that they are
269 limited to compounds with 10 oxygen atoms or lower. This limit is linked to α-pinene whose oxidation beyond 10
270 oxygen atoms remains weak (less than 2% of the detected molecules for this terpene). In the case of limonene, the
271 presence of an exocyclic double bond will increase, in a similar way to atmospheric chemistry (Kundu et al., 2012),
272 the possibilities of oxidation and accretion. It remains however impossible, considering the size of the whole dataset
273 and the diversity of the isomers, to formalize all the reaction mechanisms. Nevertheless, the formation of oxidized
274 species can be described with the help of graphical tools. The number of oxygen atoms per molecule indicates that
275 limonene oxidizes more than α-pinene (Fig. 1a). In the case of limonene, with a HESI source, chemicals with an
276 oxygen number of up to 15 were detected. Most of the chemical formulas recorded had 8-10 O-atoms (Fig. 1c), whereas
277 for α-pinene the products with >8 O-atoms were much less abundant (Fig. 1b). Moreover, for the products specific of
278 limonene oxidation, this graph shows a distribution centered on 9 oxygen atoms with carbon skeletons probably
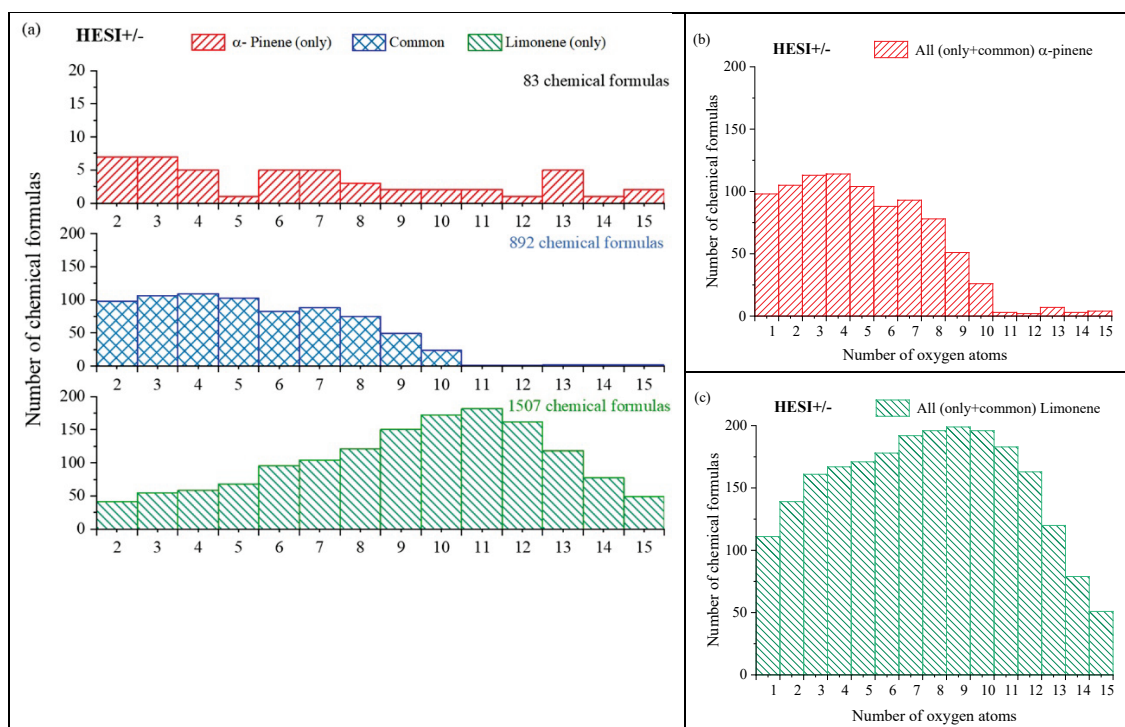279 resulting from accretion.

280

281

282

283

284

285

Figure 1. Distribution of α-pinene and limonene oxidation products as a function of their oxygen content (ionization source: HESI, combined positive and negative modes data). (a) α-pinene and limonene HESI(+/–), (b) α-pinene HESI(+/–), (c) limonene HESI(+/–)

To verify this accretion hypothesis, we can plot the OSc as a function of the number of carbon atoms or the O/C ratio at fixed number of C-atoms (Fig. 2). Indeed, the presence of chemical compounds with 11 carbon atoms can be explained by an accretion phenomenon (Wang et al., 2021), but the advantage of this OSc vs. nC space representation (Kroll et al., 2011) is to allow studying this phenomenon on all the data. One can visualize the evolution of the molecular oxidation for each carbon skeleton and the formation of oligomers. Species that are unique to one of the isomers, or common to both are differentiated using different colors. In addition, in Fig. 2a, we observe mechanisms of fragmentation ($C_{<10}$), accretion and oligomerization ($C_{>10}$). These reaction mechanisms contribute to forming chemical classes according to their number of carbon atoms, up to C=30. This limit is probably due to the ionization or detection capacity of the spectrometer. The increase in the number of oxygen atoms, but also of carbon atoms will decrease products volatility. Following a classification proposed in the literature (Kroll et al., 2011), we distinguished four sets of products: low volatile oxidized organic aerosols (LV-OOA), semi-volatile oxidized organic aerosols (SV-OOA), biomass burning organic aerosols (BBOA) and water-soluble organic carbons (WSOC). In the OSc versus carbon number plot (Fig 2a), the vertical lines (at constant carbon number) are a first criterion for finding potential candidate products of autoxidation. Figure 2b shows, for a fixed number of carbon and hydrogen atoms, the diversity of oxidized species formed. Different oxygen parities are observed, showing that different reaction mechanisms occur.
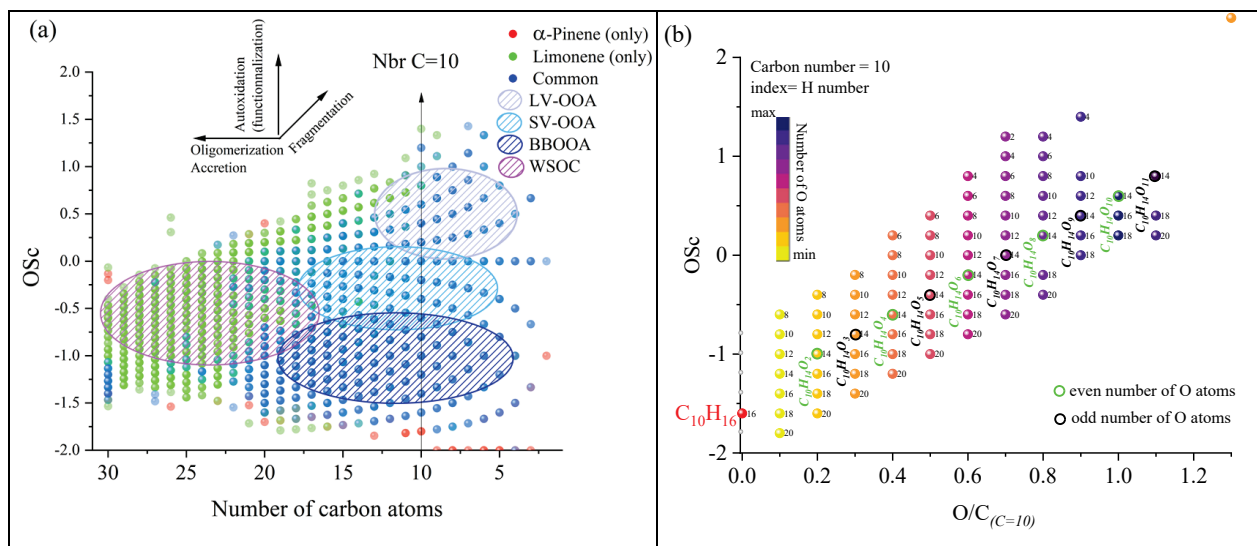
Figure 2. Overview of the distribution of limonene and α-pinene oxidation products observed in a JSR: (a) OSc versus carbon number in detected chemical formulas from APCI and HESI data. (b) Molecular formulas detected in this study presented in the OSc versus O/C space for a carbon number of 10; index of the products: number of hydrogen atoms.

This parity distinction is initially present for the two main radicals, ROO˙ and RO˙ involved in autoxidation mechanisms. However, termination and propagation reactions will change the oxygen parity (Fig. 3). Then, parity links between radicals and molecules are lost, which prevents interpretation of radical oxidation routes. HESI data showed an equivalent distribution of oxygen parities in molecular products (odd: 51%, even 49%) which cannot allow concluding on the relative importance of reaction pathways. It should be noted that other reaction mechanisms can also change oxygen parity, e.g., QOOH → cyclic ether (QO) + OH (Wang et al., 2017). Figure 2 (b) illustrates the autoxidation products presented in Fig. S3. There, one can see the formation routes to even-oxygen compounds $C_{10}H_{14}O_{2 \text{ to } 10}$ and to odd-oxygen compounds $C_{10}H_{14}O_{3 \text{ to } 11}$. The molecular formulas detected in our experiments as shown in bold in Fig. 2b. The others formulas presented in Fig. 2b should result from others oxidation pathways. Indeed, products with chemical formulas with H≥16 cannot derive from the autoxidation pathways described in Fig S3. Other pathways (Fig. S5) can yield such species, e.g., through the initial addition of OH on terpenes double bonds followed by O_2 addition and autoxidation of resulting products.
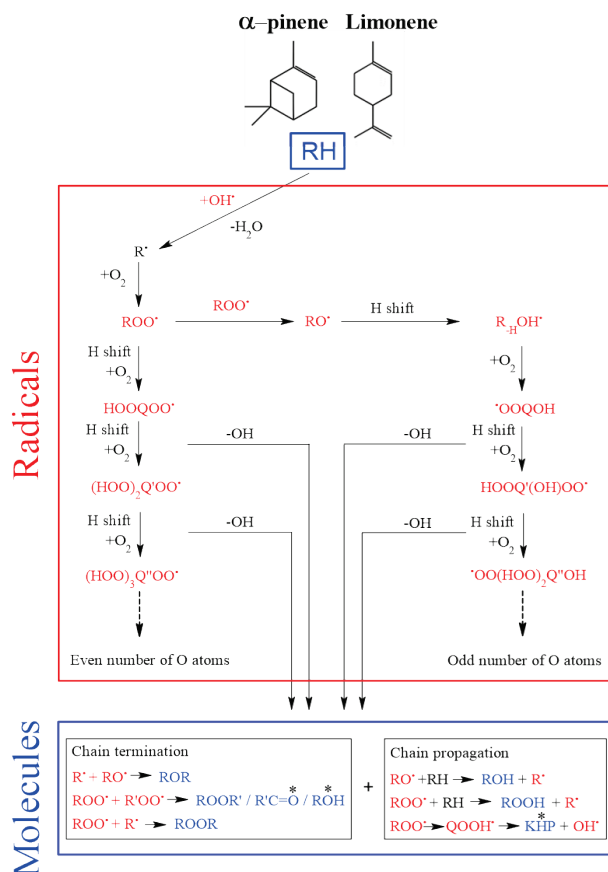
Figure 3. Accepted autoxidation reaction mechanisms in combustion (left) and in the atmosphere (left and right). * indicates a change of oxygen atoms parity (Berndt et al., 2016).

Nevertheless, despite this change in parity, in the case of autoxidation, the free-radical reaction pathway (shown in Supplements Figs. S3 and S5 for both oxygen parities) can produce a set of molecular products that mirrors repeated O_2 addition, characteristic of autoxidation (Fig. 2b). Furthermore, we studied the relative intensities of identified chemical formulas for alpha pinene and limonene (HESI source). The results presented in Table 2 show overall a decrease in relative intensities of products signal with increasing number of oxygen atoms ($C_{10}H_{14}O_{2,4,6,8...}$; $C_{10}H_{14}O_{3,5,7...}$) for both terpenes. It is clear that the repeated addition of O_2 on radicals (Fig S3) associated with the decrease of the relative intensities of the products formed is not sufficient to assess an autoxidation mechanism although it is a necessary step to constrain the identification phase of the isomers, otherwise impossible within sets composed of several thousands of chemical molecules. Finally, few chemical formulas with no chemical relevance (CxH4Oy) were detected. These are probably artefacts linked to the characterization method (ionization mode, ions transfer, ions isolation in the C-trap, incorrect masse identification). We chose to leave these data, knowing that they would be discarded in the various subsequent comparisons.

Table 2: Relative intensities of detected chemical formulas for alpha pinene and limonene (HESI– data) which could result from autoxidation of these terpenes. Signal intensities are given in parentheses. Chemical formulas are highlighted in red in the Supplementary database.

	Limonene	Alpha-pinene
Even number of oxygen atom		
hydroxyketone	$C_{10}H_{14}O_2$ (1.61442E+7)	$C_{10}H_{14}O_2$ (4.54785E+7)
+O₂ (1st)	$C_{10}H_{14}O_4$ (3.34718E+7)	$C_{10}H_{14}O_4$ (2.52885E+6)
+O₂ (2nd)	$C_{10}H_{14}O_6$ (9.58108E+6)	$C_{10}H_{14}O_6$ (7.56393E+4)
+O₂ (3rd)	$C_{10}H_{14}O_8$ (9.55306E+5)	$C_{10}H_{14}O_8$ (2.91182E+4)
+O₂ (4th)	$C_{10}H_{14}O_{10}$ (1.00597E+4)	$C_{10}H_{14}O_{10}$ (not detected)
	$C_{10}H_{14}O_{12}$ (not detected)	--
Odd number of oxygen atom		
hydroperoxy carbonyl	$C_{10}H_{14}O_3$ (3.23297E+7)	$C_{10}H_{14}O_3$ (9.3999E+6)
+O₂ (1st)	$C_{10}H_{14}O_5$ (2.27278E+7)	$C_{10}H_{14}O_5$ (1.17044E+5)
+O₂ (2nd)	$C_{10}H_{14}O_7$ (4.04207E+6)	$C_{10}H_{14}O_7$ (7.17307E+4)
+O₂ (3rd)	$C_{10}H_{14}O_9$ (1.92816E+5)	$C_{10}H_{14}O_9$ (not detected)
+O₂ (4th)	$C_{10}H_{14}O_{11}$ (6.34129E+3)	--
	$C_{10}H_{14}O_{13}$ (not detected)	--

4.3 Combustion versus atmospheric oxidation

4.3.1 Global analysis

We have explored potential chemical pathways related to autoxidation in the previous Section. For this purpose, we have performed experiments under cool flame conditions (590 K). This autoxidation mechanism is also present in atmospheric chemistry, but it is only recently that it has been found that this mechanism could be one of the main formation pathways for SOA (Savee et al., 2015;Crounse et al., 2013;Jokinen et al., 2014a;Iyer et al., 2021). Studies have described this mechanism in the case of atmospheric chemistry with the identification of radicals and molecular species (Tomaz et al., 2021). However, previous studies on the propagation of this reaction mechanism have mainly focused on the initial steps of autoxidation without screening all identified chemical formulas for potential autoxidation products. It is therefore useful to assess the proportion of possible autoxidation products among the total chemical species formed.

Here, we propose a new approach which consists in assessing a set of molecules mainly resulting from autoxidation against different sets of experimental studies related to atmospheric chemistry. The objective is to evaluate similarity of oxidation products formed under these conditions. For this purpose, we selected a HESI ionization source, better suited for detecting higher polarity oxidized molecules, as well as higher molecular weight products (detection of 96% of the total chemical formulas observed in autoxidation by APCI and HESI).

Among published atmospheric chemistry studies of terpenes oxidation, we have selected 15 studies presenting enough chemical products of oxidation, 4 for α-pinene and 11 for limonene. The data were acquired using different experimental procedures (methods of oxidation, techniques of characterization). Table 3 summarizes all the

364 experimental parameters related to the selected studies. From that Table, one can note that few studies involved
365 chromatographic analyzes (Tomaz, 2021; Witkowski an Gierczak, 2017; Warscheid and Hoffmann, 2001). The data
366 are from the articles or files provided in the Supplement Tables S1 and S2. In these studies, oxidation was performed
367 only by ozonolysis with different experimental conditions that gather the main methods described in the literature:
368 ozonolysis, dark ozonolysis, ozonolysis with OH scavenger, ozonolysis with or without seed particles. We considered
369 that the ionization mode used in mass spectrometry did not modify the nature of the chemical species but only the
370 relative detection of ions, depending on the type of ionization used, and the sensitivity of the instruments (Riva et al.,
371 2019). The combination of data obtained using (+/–) HESI gives a rather complete picture of the autoxidation products.

372 First, we compared the data from ozonolysis studies of each terpene and identified similarities through Venn diagrams.
373 For studies with two ionization sources, duplicate chemical formulas were removed. We selected the four most
374 representative studies by the number of the chemical formulas detected. Then, we compared the set of chemical
375 formulas identified after ozonolysis to those produced in low-temperature combustion, the objective being (i) to
376 highlight similarities in terms of products generated by the two oxidation modes and (ii) to identify chemicals resulting
377 from autoxidation.

378

379

Table 3. Experimental settings of 15 oxidation studies of two terpenes under atmospheric conditions and cool flames (LC stands for liquid chromatography).

| Reference	Oxidation mode	Sampling	Experimental setup	Concentrations of reactants	Ionization /source	Instrument	Chemical formulas	LC
				α-Pinene				
Y. Deng et al. (2021)	Dark ozonolysis seed particles OH scavenger	online	Teflon bag; 0.7m³	3.3±0.6 ncps ppbv⁻¹ α -Pinene	ESI	ToF-MS	351	No
Quéléver et al. (2019)	Ozonolysis	online	Teflon bag 5 m³	10 & 50 ppb α -Pinene	NO_3^- (CI)	CI-APi-TOF	68	No
Meusinger et al. (2017)	Dark Ozonolysis OH scavenger no seed particles	offline	Teflon bag 4.5 m³	60 ppb α -Pinene	Proton transfer	PTR-MS-ToF	153	No
Krechmer et al. (2016)	Ozonolysis	offline	PAM Oxidation reactor	Field measurement	ESI (−) and NO_3^- (CI)	CI-IMS-ToF	43	No
This work	Cool-flame autoxidation	offline	Jet-stirred reactor 42 ml	1%, α -pinene No ozone	APCI(3kV) HESI (3kV)	Orbitrap® Q-Exactive	820 (APCI) 975 (HESI)	Yes
				Limonene				
Krechmer et al. (2016)	Ozonolysis	offline	PAM Oxidation reactor	not specified	ESI (−) and NO_3^- (CI)	CI-IMS-ToF	63	No
Tomaz et al. (2021)	Ozonolysis	online	Flow tube reactor (18L)	45-227 ppb limonene	NO_3^- (CI) - Neg	Orbitrap® Q-Exactive	199	Yes
Fang et al. (2017)	OH-initiated photooxidation dark ozonolysis	online	Smog chamber	900–1500 ppb limonene	UV; 10 eV	Time-of-Flight (ToF)	17	No
Witkowski and Gierczak (2017)	Dark ozonolysis	offline	Flow reactor	2 ppm, limonene	ESI,4.5 kV	Triple quadrupole	12	Yes
(Jokinen et al., 2015)	Ozonolysis	online	Flow glass tube	1–10000 x10⁹ molec.cm⁻³, limonene	NO_3^- (CI)	Time-of-Flight (ToF)	11	No
Nørgaard et al. (2013)	Ozone (plasma)	online	direct on the support	850 ppb ozone 15-150 ppb limonene	plasma	Quadrupole time-of-flight (QToF)	29	No
Bateman et al. (2009)	Dark and UV radiations ozonolysis	offline	Teflon FEP reaction chamber	1 ppm ozone 1 ppm limonene	modified ESI (+/−)	LTQ-Orbitrap Hybrid Mass (ESI)	924	No
Walser et al. (2008)	Dark ozonolysis	offline	Teflon FEP reaction chamber	1-10 ppm ozone 10 ppm limonene	ESI (+/−); 4.5 kV	LTQ-Orbitrap Hybrid Mass (ESI)	465	No
Warscheid & Hoffmann (2001)	Ozonolysis	online	Smog chamber	300-500 ppb limonene	APCI; 3kV	Quadrupole ion trap mass	21	Yes
Hammes et al., (2019)	Dark ozonolysis	online	Flow reactor	15, 40, 150 ppb limonene	²¹⁰Po α acetate ions	HR-ToF-CIMS	20	No
Kundu et al. (2012)	Dark ozonolysis	offline	Teflon reaction chamber	250 ppb ozone 500 ppb limonene	ESI; 3.7 and 4 kV	LTQ FT Ultra, Thermo Sct (ESI)	1197	No
This work	Cool-flame autoxidation	offline	Jet-stirred reactor 42 ml	1%, limonene No ozone	APCI(3μA) HESI (3kV)	Orbitrap® Q-Exactive	1863(APCI) 2399(HESI)	Yes

For α-pinene oxidation, in the four selected studies 567 chemical formulas were detected, all polarities combined.

Only one study (Meusinger et al., 2017) was performed in positive ionization mode and none of the studies reported

385   data were obtained with two ionization modes (+/−). For the oxidation of limonene, the four selected studies identified

386   1434 chemical formulas. Among these studies, the experiments by Walser et al. were performed with both (+) and (−

387   ) ionization modes. In contrast to the α-pinene case, the selected studies for limonene were performed with similar

388   ionization sources, which probably contributed to increased data similarity (Walser et al., 2008). In the case of

389   limonene oxidation, for which accretion is more important than for α-pinene, and for which a greater number of

390   chemical formulas were identified, the similarities are more important (Jokinen et al., 2014b). These results are

391   presented in Figure 4 where the ionization polarity used in each study is specified.

392
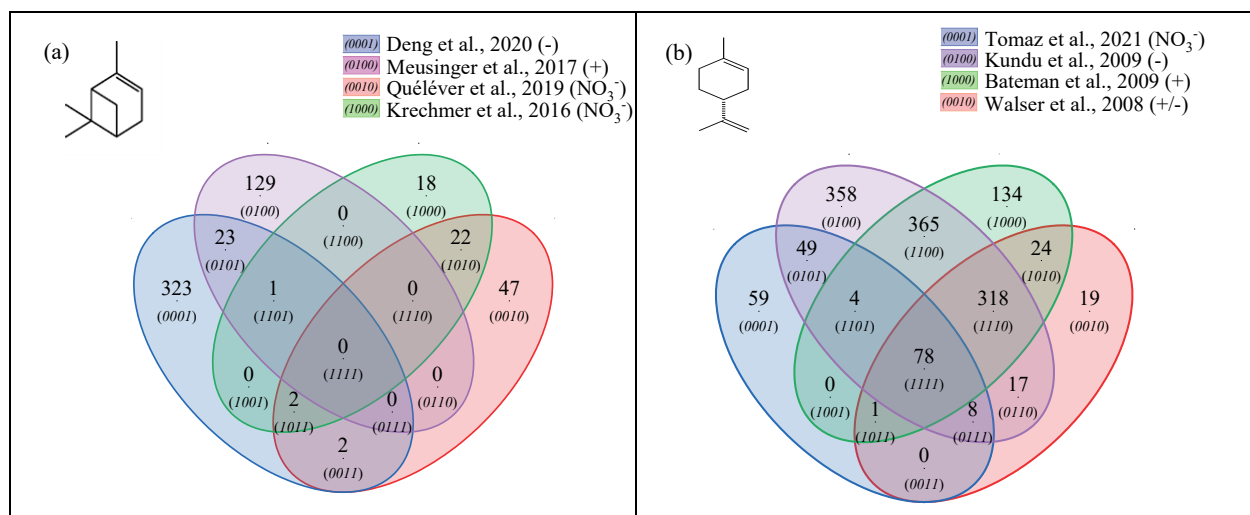
393   **Figure 4.** Venn diagrams for comparing the oxidation results from ozonolysis of (a) α-pinene and (b) limonene (see

394   conditions in Table 1). Each digit indicates a study, the value of the digit characterizes the presence (value 1) or

395   absence (0) common products detected in different studies, e.g., 23 chemical formulas (0101) (Fig. 4a) are common

396   to the studies of Deng et al; (0001) and Meusinger et al. (0100)

397   For α-pinene, no chemical formula is common to all datasets. Different hypotheses can be offered to explain this

398   result. Among them, the number of chemical formulas identified per study remains limited (a few dozen to several

399   hundred) and these small datasets are sometimes restricted to specific mass ranges, e.g. C_{10} to C_{20} (Quéléver et al.,

400   2019). In the case of studies carried out with an NO_3^- source, sensitive to HOMS, produced preferentially by

401   autoxidation, we note that nearly 50% of the chemical formulas (10/22; (*1010*)) are linked by a simple difference of 2

402   oxygen atoms.

403   For limonene, chemical formulas are common to the four studies selected here. In this data set, a large majority of

404   chemical formulas show a similar relationship to autoxidation, i.e., a simple difference of two oxygen atoms: 62%

405   (Tomaz et al., 2021), 54% (Walser et al., 2008), 69% (Kundu et al., 2012), 66% (Bateman et al., 2009) and 72% (this

406   study). This result seems to indicate that autoxidation dominates.

407   One can then ask if reaction mechanisms common to atmospheric and combustion chemistry can generate, despite of

408   radically different experimental conditions, a set of common chemical formulas and if in this common dataset, a

409   common link, characteristic of autoxidation, is observable? To address that question, we compared all the previous

410   results, for each of these terpenes to those obtained under the present combustion study. The comparisons were made

411   using our HESI data. One should remember that the oxidation conditions in the JSR were chosen in order to maximize

412   low-temperature autoxidation. Again, we used Venn diagrams to analyze these datasets consisting of 1590 chemical

413 formulas in the case of α-pinene and 5184 chemical formulas in the case of limonene. The results of these analyses

414 are presented in Figure 5.

415 It turned out that for α-pinene, 301 chemical formulas and for limonene 871 chemical formulas were common to

416 oxidation by ozonolysis (with or without scavenger) and combustion. This represents 31% of the chemical formulas

417 for the ozonolysis of α-pinene and 36% for those of limonene ozonolysis. For α-pinene, the similarities compared to

418 combustion are specific to each study: (Deng et al., 2021) 69% (243), (Meusinger et al., 2017) 46%, (71) (Quéléver et

419 al., 2019) 7% (5), (Krechmer et al., 2016) 23% (10). Chemical formulas common to all studies were not identified.

420 This lack of similarity may be due to a partial characterization of the chemical formulas, a weaker oxidation of α-

421 pinene with an ionization mode less favorable to low molecular weights products.
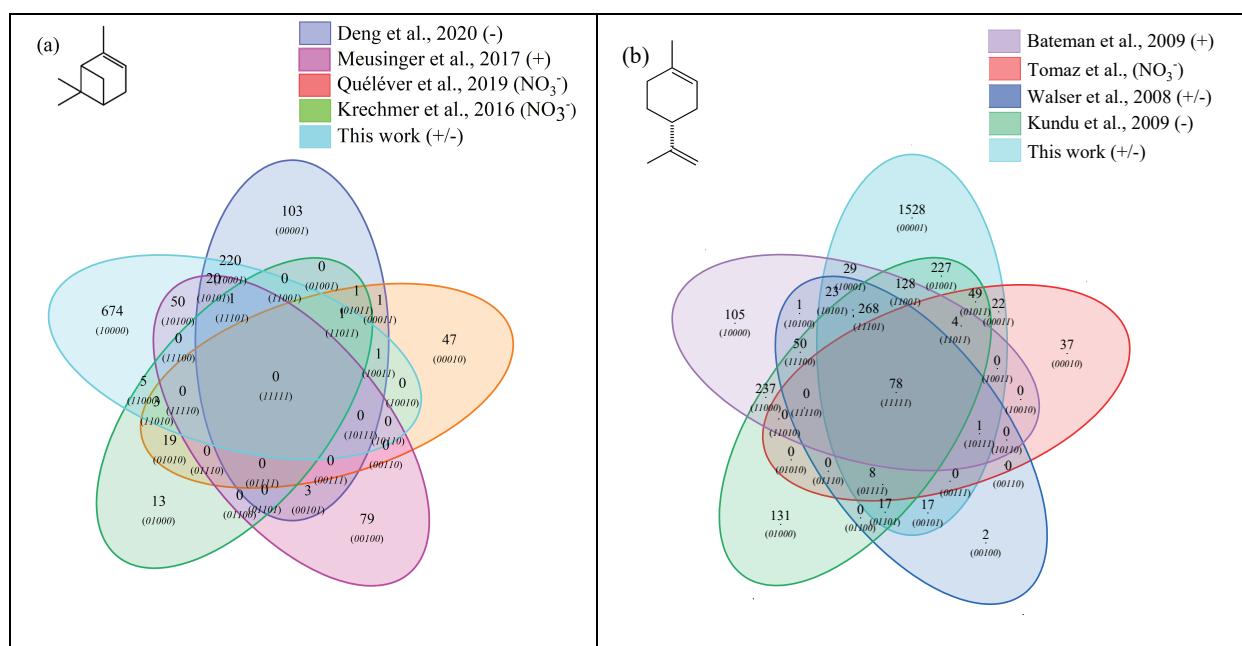
Figure 5. Venn diagrams comparing the oxidation results from ozonolysis and combustion of (a) α-pinene and (b)
limonene (see conditions in Table 1).

424 For limonene, the similarities with combustion are more important and less spread out. They represent for the different

425 studies: 65% (Kundu et al., 2012), 88% (Walser et al., 2008), 81% (Tomaz et al., 2021), and 57% (Bateman et al.,

426 2009). Moreover, there is a common dataset of 78 chemical formulas which can derive from autoxidation mechanisms.

427 Considering the very different experimental conditions, we must wonder about the impact of the double bonds in this

428 similarity. In the case of limonene, we think their presence will indeed promote the formation of allylic radicals and

429 then peroxide radicals (one of the motors of autoxidation). It is necessary to specify again that different reaction

430 mechanisms can cause the observed similarities. However, the preponderance of autoxidation in so-called cool flame

431 combustion is obvious, and in atmospheric chemistry, this reaction mechanism is competitive or dominates (Crounse

432 et al., 2013;Jokinen et al., 2014a). If we search for an autoxidation link between these 78 chemical formulas, we

433 observe that 45% of these chemical formulas meet this condition: difference of two oxygen atoms between formulas,

434 at constant number of carbon and hydrogen atoms (Data supplements, tab-5) More precisely, these molecules are

435 centered in a van Krevelen diagram on the ratios O/C=0.6 and H/C=1.6, in the range 0.29 < O/C < 0.77 and 1.33 <

436 H/C < 1.8. All oxidized molecules associated with this dataset are presented in Figure 6. The dispersion of chemical

formulae, far from being random, could be correlated with an autoxidation mechanism where the number of carbon and hydrogen atoms are constant.
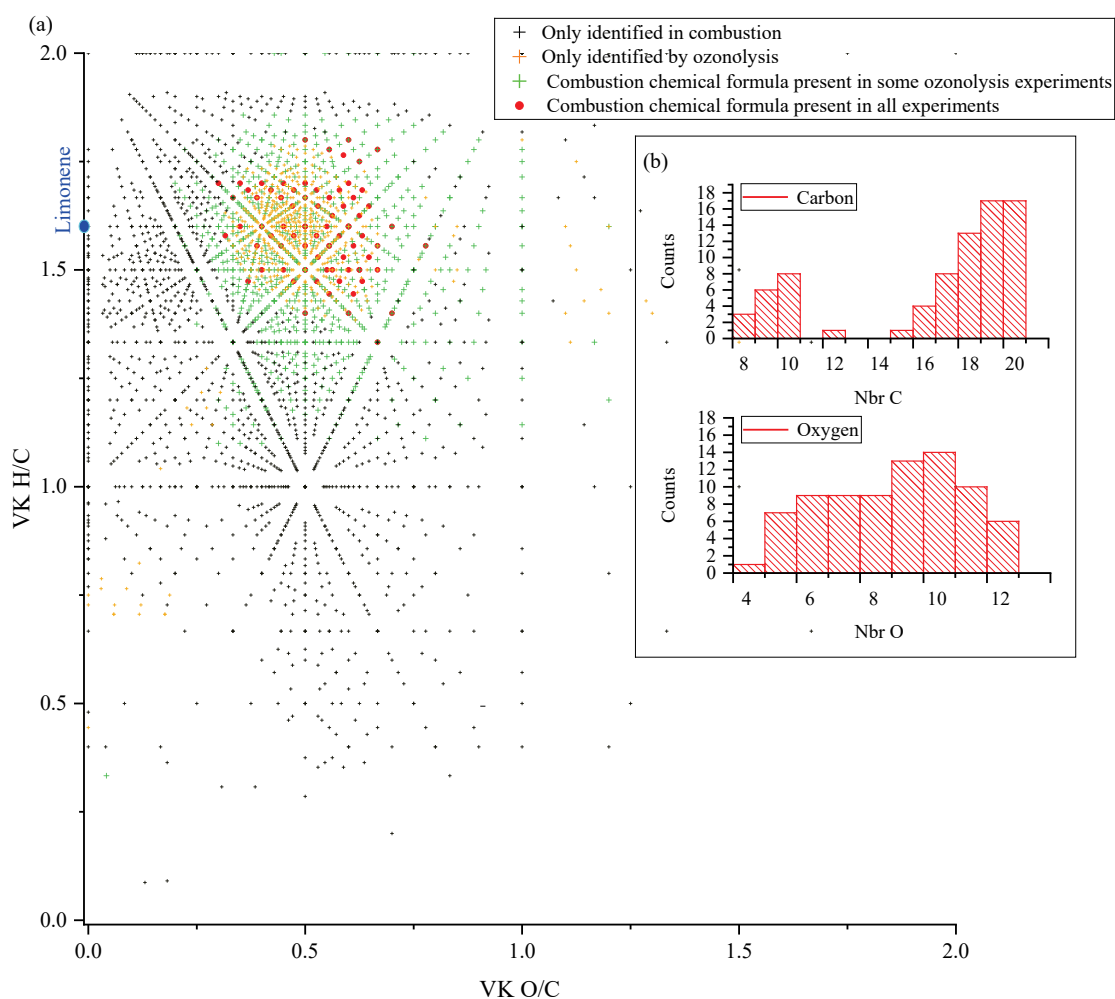

Figure 6. (a) Van Krevelen diagram showing specific and common chemical formulas detected after to oxidation of limonene by ozonolysis and combustion; insert (b): distributions of the number of carbon and oxygen atoms in the 78 chemical formulas common to all experiments.

A 3-D representation of all limonene oxidation data is given in Supplement (Fig. S4a) where DBE is used as third dimension. From that figure, one can note that products with higher DBE (DBE>10) are preferably formed under JSR conditions, i.e., at elevated temperature. A 2D representation (OSc vs DBE, Fig. S4b) completes this 3D view. The corresponding chemical formulas with DBE > 10 could correspond to carbonyls and / or cyclic ethers (˙QOOH → carbonyl + alkene + OH and / or cyclic ether + OH˙). Specificities and similarities of these two oxidation modes (ozonolysis/combustion) were further investigated by plotting the distribution of the number of oxygen atoms in detected chemical formulas (Fig. 7). Indeed, the distribution of the number of oxygen atoms allows, in addition to the Van Krevelen diagram, to provide some additional details on these two modes of oxidation. In ozonolysis, we observed the chemical formulas having the largest number of oxygen atoms. There, oxidation proceeds over a long reaction time where the phenomenon of aging appears through accretion or oligomerization. In combustion, the number of oxygen atoms remains limited to 18, with a lower number of detected chemical formulas compared to the case of ozonolysis. JSR-FIA-HRMS data indicated many more sets of chemical formulas differing by two O-atoms in the

455 range $C_{10}H_xO_{2-10}$ ($C_{10}H_{12}O_{2-10}$, $C_{10}H_{12}O_{3-9}$, $C_{10}H_{14}O_{2-10}$, $C_{10}H_{14}O_{3-9}$, $C_{10}H_{16}O_{2-8}$, $C_{10}H_{16}O_{3-9}$); see Supplementary

456 database, tab-4. Although at this stage one cannot prove these species were formed through autoxidation, their formulas

457 are consistent with autoxidation products. It is in combustion that we observed the highest O/C ratios, indicating the

458 formation of the most oxidized products. This difference, however, does not affect the similarities between the

459 chemical formulas detected in the two modes of oxidation. Finally, the analysis of the parities in oxygen atoms, very

460 similar for the three datasets, confirms that the reaction mechanisms presented in Figure 3 do not allow a simple link

461 to be established between the oxygen parity of radicals and that of the detected molecular products. The list of these

462 78 chemical formulas is given in the data-supplement file
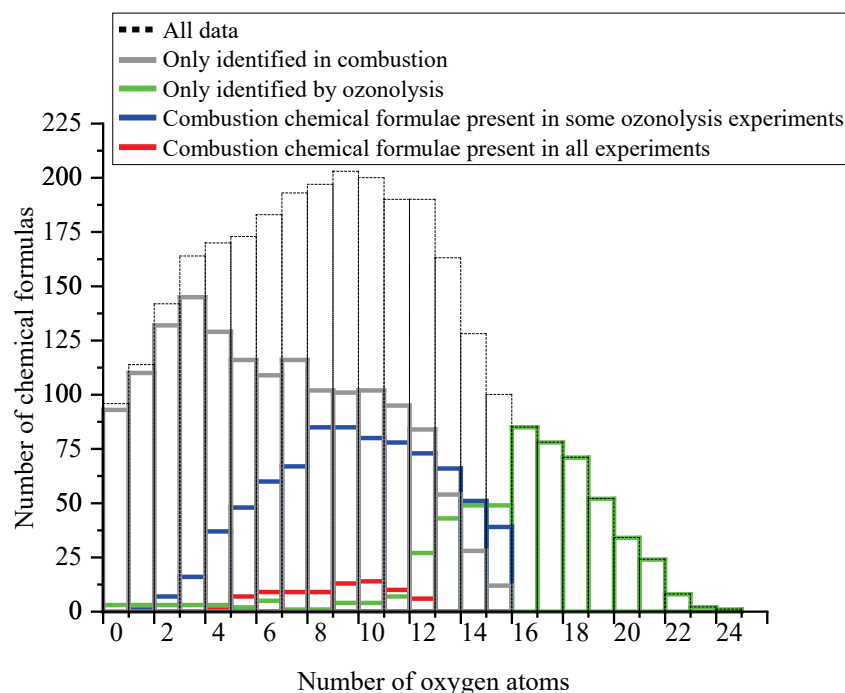
463
464 **Figure 7.** Oxygen number distribution for all the molecules identified for the oxidation of limonene: only in
465 combustion, only in ozonolysis and common to both processes.

466 *4.3.2 Identification of common isomers.*

467 We identified a set of chemical formulas common to both atmospheric and combustion oxidation modes and suggested

468 that this might result from an autoxidation mechanism. We detected several chemical formulas within this dataset that

469 differ by two oxygen atoms on the same skeleton ($C_{10}H_{16}O_x$). Some of these chemical formulas were previously

470 identified in Figure 2b or in the 78 common chemical formulas. Focusing on the early stages of limonene oxidation,

471 there are several chemical formulas, starting from $C_{10}H_{16}O_2$ and $C_{10}H_{16}O_3$, which contain increasing (by 2) number of

472 oxygen atoms. Table 4 presents the identified chemical formulas with Venn index given in parentheses and ions

473 intensity. The index for combustion is the rightmost (xxxx1).

474 Table 4. Products of multiple addition of oxygen on limonene oxidation product by OH. Chemical formulas are
475 highlighted in red in the Supplementary database.

First stages of oxidation	1st addition	2nd addition	3rd addition	4th addition	5th addition
$C_{10}H_{16}O_2$ *(10101)* 3.64425E+6	$C_{10}H_{16}O_4$ *(11101)* 1.01228E+7	$C_{10}H_{16}O_6$ *(11111)* 1.99061E+6	$C_{10}H_{16}O_8$ *(01011)* 8.62699E+4	$C_{10}H_{16}O_{10}$ *(00011)* 4.33184E+4	$C_{10}H_{16}O_{12}$ *(00010)*
$C_{10}H_{16}O_3$ *(11101)* 1.2035E+7	$C_{10}H_{16}O_5$ *(11111)* 5.91408E+6	$C_{10}H_{16}O_7$ *(11111)* 4.90565E+5	$C_{10}H_{16}O_9$ *(01011)* 2.08502E+4	$C_{10}H_{16}O_{11}$ *(00010)*	

476

477   A proposed formation route of the $C_{10}H_{16}O_x$ species is provided in the supporting (Scheme S5). As can be seen from

478   there, an autoxidation mechanism can start from $^•C_{10}H_{15}O_4$ and $^•C_{10}H_{15}O_6$, yielding odd-oxygen compounds shown in

479   Table 4. For even-oxygen compounds, one could propose they are formed after production of RO$^•$, through reaction

480   R3 (Fig. S3) or decomposition of ROOH to yield RO• and OH•, and also through oxidation of •$C_{10}H_{17}O_5$ (Fig. S5).

481   Products of additions of two oxygens are also observed for other chemical formulas within this common dataset. To

482   further investigate the possible formation of common products through atmospheric and combustion chemistries,

483   UHPLC-HRMS experiments were performed. The chemical compounds $C_{10}H_{16}O_2$ for limonene and $C_{10}H_{16}O_3$ for α-

484   pinene were selected considering the availability of standards from suppliers and were among the most frequently

485   reported products in atmospheric chemistry studies (Table 5). Our study shows same retention times for these standards

486   and isomers detected in combustion samples (Fig S6). This result is more obvious for limonoaldehyde (11.5 min) than

487   for pinonic acid (3.9 min). In addition, we detected the presence of -OH or -OOH groups by H/D exchange with D_2O

488   and C=O groups through derivatization of carbonyls with 2,4-DNPH for these two chemical formulas (Fig. S7). The

489   low intensity of H/D exchange for α-pinene oxidation products indicates that the pinonic acid isomer is probably

490   present at low concentration in the sample. Unfortunately, coelution did not fully allow exploiting MS/MS

491   fragmentation carried out on the two chemical formulas, and to formally identify the two compounds. There is still a

492   lot of characterization work to be done, but the hypothesis of common isomeric products formed through an

493   autoxidation mechanism operating in atmospheric and low-temperature combustion conditions seems to be confirmed.

494   **Table 5.** Isomers of α-pinene and limonene oxidation reported in the literature.

	$C_{10}H_{16}O_2$		$C_{10}H_{16}O_3$	
α-pinene	Pinonaldehyde	(Fang et al., 2017)	Pinonic acid	(Fang et al., 2017;Ng et al., 2011;Meusinger et al., 2017)
	hydroxyketone	(Fang et al., 2017)	hydroxy pinonaldehydes	(Fang et al., 2017;Meusinger et al., 2017)
Limonene	limononaldehyde	(Fang et al., 2017;Walser et al., 2008;Bateman et al., 2009)	limononic acid	(Fang et al., 2017;Witkowski and Gierczak, 2017;Hammes et al., 2019;Walser et al., 2008;Bateman et al., 2009;Warscheid and Hoffmann, 2001)
	4-isopropenyl-methylhydroxy-2-oxocyclohexane	(Fang et al., 2017)	7-hydroxy-limononaldehyde	(Fang et al., 2017;Walser et al., 2008;Bateman et al., 2009;Meusinger et al., 2017)

495

496   **5 Conclusion**

497   The oxidation of limonene-oxygen-nitrogen and α-pinene-oxygen-nitrogen mixtures was carried out using a jet-stirred

498   reactor at elevated temperature (590 K), a residence time of 2 s, and atmospheric pressure. The products were analyzed

499   by liquid chromatography, flow injection, and soft ionization-high resolution mass spectrometry. H/D exchange and

500   2,4-dinitrophenyl hydrazine derivatization were used to assess the presence of OOH and C=O groups in products,

501   respectively. We probed the effects of the type of ionization used in mass spectrometry analyses on the detection of

502   oxidation products. Heated electrospray ionization (HESI +/–) and atmospheric pressure chemical ionization (APCI

503   +/–) were used. A large dataset was obtained and compared with literature data obtained during the oxidation of

504   limonene and α-pinene under simulated tropospheric and low-temperature oxidation conditions. This work showed a

505 surprisingly similar set of chemical formulas of products, including oligomers, formed under the two rather different

506 conditions, i.e., cool flames and simulated atmospheric oxidation. Data analysis involving van Krevelen diagrams,

507 oxygen number distribution, oxidation state of carbon, and chemical relationship between molecules, indicated that a

508 subset of chemical formulas is common to all experiments independently of experimental conditions. More than 35%

509 of the chemical formulas detected in combustion chemistry experiments using a JSR have been detected in the studies

510 carried out under atmospheric conditions. Finally, we have outlined the existence of a substantial common dataset of

511 autoxidation products. This result tends to show that autoxidation is indeed inducing similarity between atmospheric

512 and combustion products. Detailed analysis of our data was performed by UHPLC-MS/MS of selected chemical

513 formulas observed in the literature. Nevertheless, final identification was not possible due to coelutions.

514 The present JSR data could be useful to atmospheric chemists working in the field of wildfire and/or biomass burning

515 induced air pollution. Considering that low-temperature oxidation (cool flame) products, i.e., VOCs, can be emitted

516 from biomass burning, wildfires and engine exhausts, the present data should be of interest for the atmospheric

517 chemists because they complement those obtained in atmospheric chemistry literature. It would be interesting to

518 complement the atmospheric relevant data with MS^2 analyses of products and assessment of the presence of

519 hydroperoxyl and carbonyl groups HOMs. Further MS^2 characterizations are also needed for the products observed in

520 the present work. Finally, a study of the temperature dependence of products formation would be very useful, both

521 under cool flame conditions and simulated atmospheric oxidation conditions.

522

527

528 **References**

529 Bailey, H. C., and Norrish, R. G. W.: The oxidation of hexane in the cool-flame region, Proceedings of the Royal
530   Society of London Series a-Mathematical and Physical Sciences, 212, 311-330,
531   https://doi.org/10.1098/rspa.1952.0084, 1952.
532 Bateman, A. P., Nizkorodov, S. A., Laskin, J., and Laskin, A.: Time-resolved molecular characterization of
533   limonene/ozone aerosol using high-resolution electrospray ionization mass spectrometry, Physical Chemistry
534   Chemical Physics, 11, 7931-7942, https://doi.org/10.1039/B905288G, 2009.
535 Belhadj, N., Benoit, R., Dagaut, P., Lailliau, M., Serinyel, Z., Dayma, G., Khaled, F., Moreau, B., and Foucher, F.:
536   Oxidation of di-n-butyl ether: Experimental characterization of low-temperature products in JSR and RCM,
537   Combustion and Flame, 222, 133-144, https://doi.org/10.1016/j.combustflame.2020.08.037, 2020.
538 Belhadj, N., Benoit, R., Dagaut, P., and Lailliau, M.: Experimental characterization of n-heptane low-temperature
539   oxidation products including keto-hydroperoxides and highly oxygenated organic molecules (HOMs),
540   Combustion and Flame, 224, 83-93, https://doi.org/10.1016/j.combustflame.2020.10.021, 2021a.
541 Belhadj, N., Lailliau, M., Benoit, R., and Dagaut, P.: Towards a Comprehensive Characterization of the Low-
542   Temperature Autoxidation of Di-n-Butyl Ether, Molecules, 26, 7174, 2021b.
543 Belhadj, N., Lailliau, M., Benoit, R., and Dagaut, P.: Experimental and kinetic modeling study of n-hexane
544   oxidation. Detection of complex low-temperature products using high-resolution mass spectrometry, Combustion
545   and Flame, 233, 111581, https://doi.org/10.1016/j.combustflame.2021.111581, 2021c.
546 Benoit, R., Belhadj, N., Lailliau, M., and Dagaut, P.: On the similarities and differences between the products of
547   oxidation of hydrocarbons under simulated atmospheric conditions and cool flames, Atmos. Chem. Phys., 21,
548   7845-7862, https://doi.org/10.5194/acp-21-7845-2021, 2021.
549 Benson, S. W.: The kinetics and thermochemistry of chemical oxidation with application to combustion and flames,
550   Progress in Energy and Combustion Science, 7, 125-134, https://doi.org/10.1016/0360-1285(81)90007-1, 1981.

Bernath, P., Boone, C., and Crouse, J.: Wildfire smoke destroys stratospheric ozone, Science, 375, 1292-1295, https://doi.org/10.1126/science.abm5611, 2022.

Berndt, T., Richters, S., Kaethner, R., Voigtländer, J., Stratmann, F., Sipilä, M., Kulmala, M., and Herrmann, H.: Gas-Phase Ozonolysis of Cycloalkenes: Formation of Highly Oxidized RO2 Radicals and Their Reactions with NO, NO2, SO2, and Other RO2 Radicals, The Journal of Physical Chemistry A, 119, 10336-10348, https://doi.org/10.1021/acs.jpca.5b07295, 2015.

Berndt, T., Richters, S., Jokinen, T., Hyttinen, N., Kurtén, T., Otkjær, R. V., Kjaergaard, H. G., Stratmann, F., Herrmann, H., Sipilä, M., Kulmala, M., and Ehn, M.: Hydroxyl radical-induced formation of highly oxidized organic compounds, Nat Commun, 7, 13677, https://doi.org/10.1038/ncomms13677, 2016.

Bianchi, F., Kurtén, T., Riva, M., Mohr, C., Rissanen, M. P., Roldin, P., Berndt, T., Crounse, J. D., Wennberg, P. O., Mentel, T. F., Wildt, J., Junninen, H., Jokinen, T., Kulmala, M., Worsnop, D. R., Thornton, J. A., Donahue, N., Kjaergaard, H. G., and Ehn, M.: Highly Oxygenated Organic Molecules (HOM) from Gas-Phase Autoxidation Involving Peroxy Radicals: A Key Contributor to Atmospheric Aerosol, Chemical Reviews, 119, 3472-3509, https://doi.org/10.1021/acs.chemrev.8b00395, 2019.

Burke, M., Driscoll, A., Heft-Neal, S., Xue, J., Burney, J., and Wara, M.: The changing risk and burden of wildfire in the United States, Proceedings of the National Academy of Sciences, 118, e2011048118, doi:10.1073/pnas.2011048118, 2021.

Camredon, M., Hamilton, J. F., Alam, M. S., Wyche, K. P., Carr, T., White, I. R., Monks, P. S., Rickard, A. R., and Bloss, W. J.: Distribution of gaseous and particulate organic composition during dark α-pinene ozonolysis, Atmos. Chem. Phys., https://doi.org/10, 2893-2917, https://doi.org/10.5194/acp-10-2893-2010, 2010.

Cox, R. A., and Cole, J. A.: Chemical aspects of the autoignition of hydrocarbon-air mixtures, Combust. Flame, 60, 109-123, https://doi.org/10.1016/0010-2180(85)90001-X, 1985.

Crounse, J. D., Nielsen, L. B., Jørgensen, S., Kjaergaard, H. G., and Wennberg, P. O.: Autoxidation of organic compounds in the atmosphere, J. Phys. Chem. Lett., 4, 3513, 2013.

Dagaut, P., Cathonnet, M., Rouan, J. P., Foulatier, R., Quilgars, A., Boettner, J. C., Gaillard, F., and James, H.: A jet-stirred reactor for kinetic studies of homogeneous gas-phase reactions at pressures up to ten atmospheres (≈1 MPa), Journal of Physics E: Scientific Instruments, 19, 207-209, https://doi.org/10.1088/0022-3735/19/3/009, 1986.

Dagaut, P., Cathonnet, M., Boetiner, J. C., and Gaillard, F.: Kinetic Modeling of Propane Oxidation, Combustion Science and Technology, 56, 23-63, https://doi.org/10.1080/00102208708947080, 1987.

Dagaut, P., Cathonnet, M., Boettner, J. C., and Gaillard, F.: Kinetic modeling of ethylene oxidation, Combustion and Flame, 71, 295-312, https://doi.org/10.1016/0010-2180(88)90065-X, 1988.

Deng, Y., Inomata, S., Sato, K., Ramasamy, S., Morino, Y., Enami, S., and Tanimoto, H.: Temperature and acidity dependence of secondary organic aerosol formation from α-pinene ozonolysis with a compact chamber system, Atmos. Chem. Phys., 21, 5983-6003, https://doi.org/10.5194/acp-21-5983-2021, 2021.

Ehn, M., Thornton, J. A., Kleist, E., Sipila, M., Junninen, H., Pullinen, I., Springer, M., Rubach, F., Tillmann, R., Lee, B., Lopez-Hilfiker, F., Andres, S., Acir, I. H., Rissanen, M., Jokinen, T., Schobesberger, S., Kangasluoma, J., Kontkanen, J., Nieminen, T., Kurten, T., Nielsen, L. B., Jorgensen, S., Kjaergaard, H. G., Canagaratna, M., Maso, M. D., Berndt, T., Petaja, T., Wahner, A., Kerminen, V. M., Kulmala, M., Worsnop, D. R., Wildt, J., and Mentel, T. F.: A large source of low-volatility secondary organic aerosol, Nature, 506, 476-479, https://doi.org/10.1038/nature13032, 2014.

Fang, W., Gong, L., and Sheng, L.: Online analysis of secondary organic aerosols from OH-initiated photooxidation and ozonolysis of α-pinene, β-pinene, Δ3-carene and d-limonene by thermal desorption–photoionisation aerosol mass spectrometry, Environmental Chemistry, 14, 75-90, https://doi.org/10.1071/EN16128, 2017.

Gilman, J. B., Lerner, B. M., Kuster, W. C., Goldan, P. D., Warneke, C., Veres, P. R., Roberts, J. M., de Gouw, J. A., Burling, I. R., and Yokelson, R. J.: Biomass burning emissions and potential air quality impacts of volatile organic compounds and other trace gases from fuels common in the US, Atmos. Chem. Phys., 15, 13915-13938, https://doi.org/10.5194/acp-15-13915-2015, 2015.

Hammes, J., Lutz, A., Mentel, T., Faxon, C., and Hallquist, M.: Carboxylic acids from limonene oxidation by ozone and hydroxyl radicals: insights into mechanisms derived using a FIGAERO-CIMS, Atmos. Chem. Phys., 19, 13037-13052, https://doi.org/10.5194/acp-19-13037-2019, 2019.

Harvey, B. G., Wright, M. E., and Quintana, R. L.: High-Density Renewable Fuels Based on the Selective Dimerization of Pinenes, Energy Fuels, 24, 267-273, https://doi.org/10.1021/ef900799c, 2010.

Harvey, B. G., Merriman, W. W., and Koontz, T. A.: High-Density Renewable Diesel and Jet Fuels Prepared from Multicyclic Sesquiterpanes and a 1-Hexene-Derived Synthetic Paraffinic Kerosene, Energy Fuels, 29, 2431-2436, https://doi.org/10.1021/ef5027746, 2015.

Hatch, L. E., Jen, C. N., Kreisberg, N. M., Selimovic, V., Yokelson, R. J., Stamatis, C., York, R. A., Foster, D., Stephens, S. L., Goldstein, A. H., and Barsanti, K. C.: Highly Speciated Measurements of Terpenoids Emitted from Laboratory and Mixed-Conifer Forest Prescribed Fires, Environmental Science & Technology, 53, 9418-9428, https://doi.org/10.1021/acs.est.9b02612, 2019.

611 Hecht, E. S., Scigelova, M., Eliuk, S., and Makarov, A.: Fundamentals and Advances of Orbitrap Mass
612   Spectrometry, Encyclopedia of Analytical Chemistry, 1-40, https://doi.org/10.1002/9780470027318.a9309.pub2,
613   2019.

614 Hu, Y., Fernandez-Anez, N., Smith, T. E. L., and Rein, G.: Review of emissions from smouldering peat fires and
615   their contribution to regional haze episodes, International Journal of Wildland Fire, 27, 293-312,
616   https://doi.org/10.1071/WF17084, 2018.

617 Huang, W., Saathoff, H., Pajunoja, A., Shen, X., Naumann, K. H., Wagner, R., Virtanen, A., Leisner, T., and Mohr,
618   C.: α-Pinene secondary organic aerosol at low temperature: chemical composition and implications for particle
619   viscosity, Atmos. Chem. Phys., 18, 2883-2898, https://doi.org/10.5194/acp-18-2883-2018, 2018.

620 Iyer, S., Rissanen, M. P., Valiev, R., Barua, S., Krechmer, J. E., Thornton, J., Ehn, M., and Kurtén, T.: Molecular
621   mechanism for rapid autoxidation in α-pinene ozonolysis, Nature Communications, 12, 878,
622   https://doi.org/10.1038/s41467-021-21172-w, 2021.

623 Jokinen, T., Sipilä, M., Richters, S., Kerminen, V.-M., Paasonen, P., Stratmann, F., Worsnop, D., Kulmala, M., Ehn,
624   M., Herrmann, H., and Berndt, T.: Rapid Autoxidation Forms Highly Oxidized RO2 Radicals in the Atmosphere,
625   Angewandte Chemie International Edition, 53, 14596-14600, https://doi.org/10.1002/anie.201408566, 2014a.

626 Jokinen, T., Sipila, M., Richters, S., Kerminen, V. M., Paasonen, P., Stratmann, F., Worsnop, D., Kulmala, M., Ehn,
627   M., and Herrmann, H.: Rapid autoxidation forms highly oxidized RO2 radicals in the atmosphere, Angew.
628   Chem., Int. Ed., 53, 14596, 2014b.

629 Jokinen, T., Berndt, T., Makkonen, R., Kerminen, V.-M., Junninen, H., Paasonen, P., Stratmann, F., Herrmann, H.,
630   Guenther, A. B., Worsnop, D. R., Kulmala, M., Ehn, M., and Sipilä, M.: Production of extremely low volatile
631   organic compounds from biogenic emissions: Measured yields and atmospheric implications, Proceedings of the
632   National Academy of Sciences, 112, 7123-7128, https://doi.org/10.1073/pnas.1423977112, 2015.

633 Kekäläinen, T., Pakarinen, J. M. H., Wickström, K., Lobodin, V. V., McKenna, A. M., and Jänis, J.: Compositional
634   Analysis of Oil Residues by Ultrahigh-Resolution Fourier Transform Ion Cyclotron Resonance Mass
635   Spectrometry, Energy Fuels, 27, 2002-2009, https://doi.org/10.1021/ef301762v, 2013.

636 Khaykin, S., Legras, B., Bucci, S., Sellitto, P., Isaksen, L., Tencé, F., Bekki, S., Bourassa, A., Rieger, L., Zawada,
637   D., Jumelet, J., and Godin-Beekmann, S.: The 2019/20 Australian wildfires generated a persistent smoke-charged
638   vortex rising up to 35 km altitude, Communications Earth & Environment, 1, 22, https://doi.org/10.1038/s43247-
639   020-00022-5, 2020.

640 Kobziar, L. N., Pingree, M. R. A., Larson, H., Dreaden, T. J., Green, S., and Smith, J. A.: Pyroaerobiology: the
641   aerosolization and transport of viable microbial life by wildland fire, Ecosphere, 9, e02507,
642   https://doi.org/10.1002/ecs2.2507, 2018.

643 Korcek, S., Ingold, K. U., Chenier, J. H. B., and Howard, J. A.: Absolute rate constants for hydrocarbon autoxidation
644   .21. Activation-energies for propagation and correlation of propagation rate constants with carbon-hydrogen bond
645   strengths, Canadian Journal of Chemistry, 50, 2285-&, https://doi.org/10.1139/v72-365, 1972.

646 Kourtchev, I., Doussin, J. F., Giorio, C., Mahon, B., Wilson, E. M., Maurin, N., Pangui, E., Venables, D. S., Wenger,
647   J. C., and Kalberer, M.: Molecular Composition of Fresh and Aged Secondary Organic Aerosol from a Mixture
648   of Biogenic Volatile Compounds: A High-Resolution Mass Spectrometry Study, Atmos. Chem. Phys., 15, 5683,
649   2015.

650 Krechmer, J. E., Groessl, M., Zhang, X., Junninen, H., Massoli, P., Lambe, A. T., Kimmel, J. R., Cubison, M. J.,
651   Graf, S., Lin, Y. H., Budisulistiorini, S. H., Zhang, H., Surratt, J. D., Knochenmuss, R., Jayne, J. T., Worsnop, D.
652   R., Jimenez, J. L., and Canagaratna, M. R.: Ion mobility spectrometry–mass spectrometry (IMS–MS) for on- and
653   offline analysis of atmospheric gas and aerosol species, Atmos. Meas. Tech., 9, 3245-3262,
654   https://doi.org/10.5194/amt-9-3245-2016, 2016.

655 Kristensen, K., Watne, Å. K., Hammes, J., Lutz, A., Petäjä, T., Hallquist, M., Bilde, M., and Glasius, M.: High-
656   Molecular Weight Dimer Esters Are Major Products in Aerosols from α-Pinene Ozonolysis and the Boreal
657   Forest, Environmental Science & Technology Letters, 3, 280-285, https://doi.org/10.1021/acs.estlett.6b00152,
658   2016.

659 Kroll, J. H., Donahue, N. M., Jimenez, J. L., Kessler, S. H., Canagaratna, M. R., Wilson, K. R., Altieri, K. E.,
660   Mazzoleni, L. R., Wozniak, A. S., Bluhm, H., Mysak, E. R., Smith, J. D., Kolb, C. E., and Worsnop, D. R.:
661   Carbon oxidation state as a metric for describing the chemistry of atmospheric organic aerosol, Nature
662   Chemistry, 3, 133-139, https://doi.org/10.1038/nchem.948, 2011.

663 Kundu, S., Fisseha, R., Putman, A. L., Rahn, T. A., and Mazzoleni, L. R.: High molecular weight SOA formation
664   during limonene ozonolysis: insights from ultrahigh-resolution FT-ICR mass spectrometry characterization,
665   Atmos. Chem. Phys., 12, 5523-5536, https://doi.org/10.5194/acp-12-5523-2012, 2012.

666 Kurtén, T., Rissanen, M. P., Mackeprang, K., Thornton, J. A., Hyttinen, N., Jørgensen, S., Ehn, M., and Kjaergaard,
667   H. G.: Computational Study of Hydrogen Shifts and Ring-Opening Mechanisms in α-Pinene Ozonolysis
668   Products, The Journal of Physical Chemistry A, 119, 11366-11375, https://doi.org/10.1021/acs.jpca.5b08948,
669   2015.

Melendez-Perez, J. J., Martínez-Mejia, M. J., and Eberlin, M. N.: A reformulated aromaticity index equation under consideration for non-aromatic and non-condensed aromatic cyclic carbonyl compounds, Organic Geochemistry, 95, 29-33, https://doi.org/10.1016/j.orggeochem.2016.02.002, 2016.

Meusinger, C., Dusek, U., King, S. M., Holzinger, R., Rosenørn, T., Sperlich, P., Julien, M., Remaud, G. S., Bilde, M., Röckmann, T., and Johnson, M. S.: Chemical and isotopic composition of secondary organic aerosol generated by α-pinene ozonolysis, Atmos. Chem. Phys., 17, 6373-6391, https://doi.org/10.5194/acp-17-6373-2017, 2017.

Mewalal, R., Rai, D. K., Kainer, D., Chen, F., Külheim, C., Peter, G. F., and Tuskan, G. A.: Plant-Derived Terpenes: A Feedstock for Specialty Biofuels, Trends Biotechnol., 35, 227-240, https://doi.org/10.1016/j.tibtech.2016.08.003, 2017.

Ng, N. L., Canagaratna, M. R., Jimenez, J. L., Chhabra, P. S., Seinfeld, J. H., and Worsnop, D. R.: Changes in organic aerosol composition with aging inferred from aerosol mass spectra, Atmos. Chem. Phys., 11, 6465-6474, https://doi.org/10.5194/acp-11-6465-2011, 2011.

Nørgaard, A. W., Vibenholt, A., Benassi, M., Clausen, P. A., and Wolkoff, P.: Study of Ozone-Initiated Limonene Reaction Products by Low Temperature Plasma Ionization Mass Spectrometry, Journal of The American Society for Mass Spectrometry, 24, https://doi.org/1090-1096, 10.1007/s13361-013-0648-3, 2013.

Nozière, B., Kalberer, M., Claeys, M., Allan, J., D'Anna, B., Decesari, S., Finessi, E., Glasius, M., Grgić, I., Hamilton, J. F., Hoffmann, T., Iinuma, Y., Jaoui, M., Kahnt, A., Kampf, C. J., Kourtchev, I., Maenhaut, W., Marsden, N., Saarikoski, S., Schnelle-Kreis, J., Surratt, J. D., Szidat, S., Szmigielski, R., and Wisthaler, A.: The Molecular Identification of Organic Compounds in the Atmosphere: State of the Art and Challenges, Chemical Reviews, 115, 3919-3983, https://doi.org/10.1021/cr5003485, 2015.

Otkjær, R. V., Jakobsen, H. H., Tram, C. M., and Kjaergaard, H. G.: Calculated Hydrogen Shift Rate Constants in Substituted Alkyl Peroxy Radicals, The Journal of Physical Chemistry A, 122, 8665-8673, https://doi.org/10.1021/acs.jpca.8b06223, 2018.

Popovicheva, O. B., Engling, G., Ku, I. T., Timofeev, M. A., and Shonija, N. K.: Aerosol Emissions from Long-lasting Smoldering of Boreal Peatlands: Chemical Composition, Markers, and Microstructure, Aerosol and Air Quality Research, 19, 484-503, https://doi.org/10.4209/aaqr.2018.08.0302, 2019.

Prichard, S. J., O'Neill, S. M., Eagle, P., Andreu, A. G., Drye, B., Dubowy, J., Urbanski, S., and Strand, T. M.: Wildland fire emission factors in North America: synthesis of existing data, measurement needs and management applications, International Journal of Wildland Fire, 29, 132-147, https://doi.org/10.1071/WF19066, 2020.

Quéléver, L. L. J., Kristensen, K., Normann Jensen, L., Rosati, B., Teiwes, R., Daellenbach, K. R., Peräkylä, O., Roldin, P., Bossi, R., Pedersen, H. B., Glasius, M., Bilde, M., and Ehn, M.: Effect of temperature on the formation of highly oxygenated organic molecules (HOMs) from alpha-pinene ozonolysis, Atmos. Chem. Phys., 19, 7609-7625, https://doi.org/10.5194/acp-19-7609-2019, 2019.

Riva, M., Rantala, P., Krechmer, J. E., Peräkylä, O., Zhang, Y., Heikkinen, L., Garmash, O., Yan, C., Kulmala, M., Worsnop, D., and Ehn, M.: Evaluating the performance of five different chemical ionization techniques for detecting gaseous oxygenated organic species, Atmos. Meas. Tech., 12, 2403-2421, https://doi.org/10.5194/amt-12-2403-2019, 2019.

Savee, J. D., Papajak, E., Rotavera, B., Huang, H., Eskola, A. J., Welz, O., Sheps, L., Taatjes, C. A., Zádor, J., and Osborn, D. L.: Carbon radicals. Direct observation and kinetics of a hydroperoxyalkyl radical (QOOH), Science, 347, 643-646, https://doi.org/10.1126/science.aaa1495, 2015.

Schneider, E., Czech, H., Popovicheva, O., Lütdke, H., Schnelle-Kreis, J., Khodzher, T., Rüger, C. P., and Zimmermann, R.: Molecular Characterization of Water-Soluble Aerosol Particle Extracts by Ultrahigh-Resolution Mass Spectrometry: Observation of Industrial Emissions and an Atmospherically Aged Wildfire Plume at Lake Baikal, ACS Earth and Space Chemistry, 6, 1095-1107, https://doi.org/10.1021/acsearthspacechem.2c00017, 2022.

Seinfeld, J. H., and Pandis, S. N.: Atmospheric Chemistry and Physics: From Air Pollution to Climate Change, 2nd ed., Wiley-Interscience, Hoboken, NJ, 1232 pp., 2006.

Smith, J. S., Laskin, A., and Laskin, J.: Molecular Characterization of Biomass Burning Aerosols Using High-Resolution Mass Spectrometry, Analytical Chemistry, 81, 1512-1521, https://doi.org/10.1021/ac8020664, 2009.

Tomaz, S., Wang, D., Zabalegui, N., Li, D., Lamkaddam, H., Bachmeier, F., Vogel, A., Monge, M. E., Perrier, S., Baltensperger, U., George, C., Rissanen, M., Ehn, M., El Haddad, I., and Riva, M.: Structures and reactivity of peroxy radicals and dimeric products revealed by online tandem mass spectrometry, Nature Communications, 12, 300, https://doi.org/10.1038/s41467-020-20532-2, 2021.

Tröstl, J., Chuang, W. K., Gordon, H., Heinritzi, M., Yan, C., Molteni, U., Ahlm, L., Frege, C., Bianchi, F., Wagner, R., Simon, M., Lehtipalo, K., Williamson, C., Craven, J. S., Duplissy, J., Adamov, A., Almeida, J., Bernhammer, A.-K., Breitenlechner, M., Brilke, S., Dias, A., Ehrhart, S., Flagan, R. C., Franchin, A., Fuchs, C., Guida, R., Gysel, M., Hansel, A., Hoyle, C. R., Jokinen, T., Junninen, H., Kangasluoma, J., Keskinen, H., Kim, J., Krapf, M., Kürten, A., Laaksonen, A., Lawler, M., Leiminger, M., Mathot, S., Möhler, O., Nieminen, T., Onnela, A., Petäjä, T., Piel, F. M., Miettinen, P., Rissanen, M. P., Rondo, L., Sarnela, N., Schobesberger, S., Sengupta, K., Sipilä, M., Smith, J. N., Steiner, G., Tomè, A., Virtanen, A., Wagner, A. C., Weingartner, E., Wimmer, D.,

Winkler, P. M., Ye, P., Carslaw, K. S., Curtius, J., Dommen, J., Kirkby, J., Kulmala, M., Riipinen, I., Worsnop, D. R., Donahue, N. M., and Baltensperger, U.: The role of low-volatility organic compounds in initial particle growth in the atmosphere, Nature, 533, 527-531, https://doi.org/10.1038/nature18271, 2016.

Van Krevelen, D. W.: Graphical-statistical method for the study of structure and reaction processes of coal, Fuel, 29, 269-284, 1950.

Vereecken, L., Müller, J. F., and Peeters, J.: Low-volatility poly-oxygenates in the OH-initiated atmospheric oxidation of α-pinene: impact of non-traditional peroxyl radical chemistry, Physical Chemistry Chemical Physics, 9, 5241-5248, https://doi.org/10.1039/B708023A, 2007.

Walser, M. L., Desyaterik, Y., Laskin, J., Laskin, A., and Nizkorodov, S. A.: High-resolution mass spectrometric analysis of secondary organic aerosol produced by ozonation of limonene, Physical Chemistry Chemical Physics, 10, 1009-1022, https://doi.org/10.1039/B712620D, 2008.

Wang, Z., Popolan-Vaida, D. M., Chen, B., Moshammer, K., Mohamed, S. Y., Wang, H., Sioud, S., Raji, M. A., Kohse-Höinghaus, K., Hansen, N., Dagaut, P., Leone, S. R., and Sarathy, S. M.: Unraveling the structure and chemical mechanisms of highly oxygenated intermediates in oxidation of organic compounds, Proceedings of the National Academy of Sciences, 114, 13102-13107, https://doi.org/10.1073/pnas.1707564114, 2017.

Wang, Z., Chen, B., Moshammer, K., Popolan-Vaida, D. M., Sioud, S., Shankar, V. S. B., Vuilleumier, D., Tao, T., Ruwe, L., Bräuer, E., Hansen, N., Dagaut, P., Kohse-Höinghaus, K., Raji, M. A., and Sarathy, S. M.: n-Heptane cool flame chemistry: Unraveling intermediate species measured in a stirred reactor and motored engine, Combustion and Flame, 187, 199-216, https://doi.org/10.1016/j.combustflame.2017.09.003, 2018.

Wang, Z., Ehn, M., Rissanen, M. P., Garmash, O., Quéléver, L., Xing, L., Monge Palacios, M., Rantala, P., Donahue, N. M., Berndt, T., and Sarathy, M.: - Efficient alkane oxidation under combustion engine and atmospheric conditions, Communications Chemistry, 4, 18, https://doi.org/10.1038/s42004-020-00445-3, 2021.

Warscheid, B., and Hoffmann, T.: Structural elucidation of monoterpene oxidation products by ion trap fragmentation using on-line atmospheric pressure chemical ionisation mass spectrometry in the negative ion mode, Rapid Communications in Mass Spectrometry, 15, 2259-2272, https://doi.org/10.1002/rcm.504, 2001.

Witkowski, B., and Gierczak, T.: Characterization of the limonene oxidation products with liquid chromatography coupled to the tandem mass spectrometry, Atmospheric Environment, 154, 297-307, https://doi.org/10.1016/j.atmosenv.2017.02.005, 2017.

Wotton, B. M., Gould, J. S., McCaw, W. L., Cheney, N. P., and Taylor, S. W.: Flame temperature and residence time of fires in dry eucalypt forest, International Journal of Wildland Fire, 21, 270-281, https://doi.org/10.1071/WF10127, 2012.

Xie, Q., Su, S., Chen, S., Xu, Y., Cao, D., Chen, J., Ren, L., Yue, S., Zhao, W., Sun, Y., Wang, Z., Tong, H., Su, H., Cheng, Y., Kawamura, K., Jiang, G., Liu, C. Q., and Fu, P.: Molecular characterization of firework-related urban aerosols using Fourier transform ion cyclotron resonance mass spectrometry, Atmos. Chem. Phys., 20, 6803-6820, https://doi.org/10.5194/acp-20-6803-2020, 2020.

Zhang, H., Yee, L. D., Lee, B. H., Curtis, M. P., Worton, D. R., Isaacman-VanWertz, G., Offenberg, J. H., Lewandowski, M., Kleindienst, T. E., Beaver, M. R., Holder, A. L., Lonneman, W. A., Docherty, K. S., Jaoui, M., Pye, H. O. T., Hu, W., Day, D. A., Campuzano-Jost, P., Jimenez, J. L., Guo, H., Weber, R. J., de Gouw, J., Koss, A. R., Edgerton, E. S., Brune, W., Mohr, C., Lopez-Hilfiker, F. D., Lutz, A., Kreisberg, N. M., Spielman, S. R., Hering, S. V., Wilson, K. R., Thornton, J. A., and Goldstein, A. H.: Monoterpenes are the largest source of summertime organic aerosol in the southeastern United States, Proceedings of the National Academy of Sciences, 115, 2038-2043, https://doi.org/10.1073/pnas.1717513115, 2018.

Zhao, Y., Thornton, J. A., and Pye, H. O. T.: Quantitative constraints on autoxidation and dimer formation from direct probing of monoterpene-derived peroxy radical chemistry, Proc Natl Acad Sci U S A, 115, 12142-12147, https://doi.org/10.1073/pnas.1812147115, 2018.